AEM
Journals.ASM.org

Aerobic Hydrogen Production via Nitrogenase in *Azotobacter vinelandii* CA6

Jesse Noar,[a] Telisa Loveless,[c] José Luis Navarro-Herrero,[d] Jonathan W. Olson,[b] José M. Bruno-Bárcena[a]

Departments of Plant and Microbial Biology[a] and Biological Sciences,[b] North Carolina State University, Raleigh, North Carolina, USA; USDA ARS-NCSU, Raleigh, North Carolina, USA[c]; Department of Automatic and Systems Engineering, Polytechnic University of Valencia, Valencia, Spain[d]

The diazotroph *Azotobacter vinelandii* possesses three distinct nitrogenase isoenzymes, all of which produce molecular hydrogen as a by-product. In batch cultures, *A. vinelandii* strain CA6, a mutant of strain CA, displays multiple phenotypes distinct from its parent: tolerance to tungstate, impaired growth and molybdate transport, and increased hydrogen evolution. Determining and comparing the genomic sequences of strains CA and CA6 revealed a large deletion in CA6's genome, encompassing genes related to molybdate and iron transport and hydrogen reoxidation. A series of iron uptake analyses and chemostat culture experiments confirmed iron transport impairment and showed that the addition of fixed nitrogen (ammonia) resulted in cessation of hydrogen production. Additional chemostat experiments compared the hydrogen-producing parameters of different strains: in iron-sufficient, tungstate-free conditions, strain CA6's yields were identical to those of a strain lacking only a single hydrogenase gene. However, in the presence of tungstate, CA6 produced several times more hydrogen. *A. vinelandii* may hold promise for developing a novel strategy for production of hydrogen as an energy compound.

Azotobacter vinelandii fixes nitrogen gas using three genetically distinct nitrogenase complexes. The primary complex is the molybdenum (Mo)- and iron (Fe)-containing enzyme that corresponds to the nitrogenase found in all diazotrophs so far characterized (1). The second is a vanadium (V)- and Fe-containing nitrogenase that is expressed under Mo-deficient conditions in the presence of V. The third nitrogenase contains only iron (1), and wild-type *A. vinelandii* strains produce it only under Mo- and V-deficient conditions (2, 3). Concentrations of Mo as low as 50 nM induce repression of the vanadium and iron-only nitrogenases in the wild type (3–6).

A. vinelandii strain CA6, an offspring of strain CA, is a mutant strain that Paul Bishop and colleagues isolated by selecting for its ability to fix nitrogen in the presence of tungstate levels that restrict the growth of the parent (7). Tungsten replaces molybdenum as the central cofactor of the primary Mo nitrogenase, rendering it nonfunctional (8). Further study revealed that CA6 expresses the alternative nitrogenase systems even in the presence of molybdate or tungstate (these compounds induce repression of the alternative nitrogenases in CA) and also showed that CA6 exhibits impaired molybdate uptake (9).

In addition, molecular hydrogen accumulation was observed in cultures of CA6 growing under nitrogen-fixing conditions. While all characterized nitrogenases produce molecular hydrogen as a by-product, the iron-only nitrogenase generates greater amounts of molecular hydrogen for each molecule of N_2 fixed than the molybdenum nitrogenase (4, 10). Wild-type *A. vinelandii* possesses a membrane-bound uptake hydrogenase which reoxidizes hydrogen that nitrogenases produce, recovering the energy rather than allowing the gas to evolve (11–14). When this hydrogenase is nonfunctional, hydrogen evolution is observed (11, 15).

Preliminary observations of CA6 raised the question of whether the strain could be considered a good catalyst for producing substantial amounts of hydrogen, a molecule that has been a focus recently as an energy-rich, clean potential biofuel (16, 17). Most biohydrogen production strategies fall into two general categories: phototrophic or fermentative (18). As an aerobic heterotrophic hydrogen producer, *A. vinelandii* would require neither the surface area that phototrophs need to collect light nor the anaerobic conditions needed for many fermentations, which could be advantageous for certain applications.

Prior to this study, it remained unclear why CA6 evolves hydrogen rather than reassimilating it. Therefore, to discover the genetic differences between the mutant *A. vinelandii* CA6 and its parent CA, we sequenced the genomes of CA and CA6 using next-generation sequencing technologies and assembled the genomes by mapping to the reference genome of *A. vinelandii* strain DJ. We performed batch and tightly controlled aerobic, carbon-limiting chemostat culture experiments and calculated associated kinetic and yield parameters to further evaluate the strains' physiological differences, including CA6's hydrogen evolution phenotype. Understanding these mechanisms could allow the evaluation and later optimization of processes utilizing *A. vinelandii* or species like it as a novel alternative for microbial molecular hydrogen production.

MATERIALS AND METHODS

Strains and medium. Figure 1 displays the strains utilized in this study and their parent-offspring relationships. CA and DJ are available from the American Type Culture Collection under numbers 13705 and BAA-1303, respectively; R.L. Robson generously shared a culture of HS2, and CA6 is

Received 3 March 2015 Accepted 20 April 2015
Accepted manuscript posted online 24 April 2015
Citation Noar J, Loveless T, Navarro-Herrero JL, Olson JW, Bruno-Bárcena JM. 2015. Aerobic hydrogen production via nitrogenase in *Azotobacter vinelandii* CA6. Appl Environ Microbiol 81:4507–4516. doi:10.1128/AEM.00679-15.
Editor: M. J. Pettinari
Address correspondence to José M. Bruno-Bárcena, jbbarcen@ncsu.edu.
Supplemental material for this article may be found at http://dx.doi.org/10.1128/AEM.00679-15.

doi:10.1128/AEM.00679-15

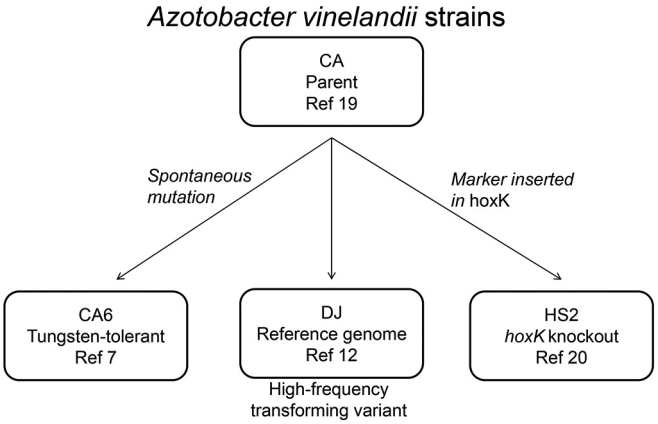

FIG 1 Strains of *A. vinelandii* used in this study. Arrows indicate direction of parent-offspring relationship.

part of NCSU's Department of Plant and Microbial Biology Culture Collection (7, 19, 20).

Azotobacter vinelandii strains were grown in modified nitrogen-free Burk broth (21); unless otherwise noted, it contained, per liter, 0.2 g $MgSO_4 \cdot 7H_2O$, 90 mg $CaCl_2 \cdot 2H_2O$, 0.25 mg $NaMoO_4 \cdot 2H_2O$, 0.2 g KH_2PO_4, 0.8 g K_2HPO_4, 2.5 mg $FeSO_4 \cdot 7H_2O$, 2.5 mg ferric citrate, and 20 g sucrose. Sucrose and iron solutions were filter sterilized with 0.2-μm-pore-size filters; other solutions were autoclaved and the various components were combined as needed. Inocula were cultured by incubating at 30°C and shaking at 200 rpm. For solid medium, agar was added to 1.5% (wt/vol).

Genomes and DNA sequencing. Hundred-milliliter cultures of CA and CA6 were divided into 5 aliquots each and pelleted. The pellets were stored at −80°C. Bacterial pellets were sent to the University of North Carolina—Chapel Hill's Microbiome Core Facility (Chapel Hill, NC) for pyrosequencing on a Roche 454 GS FLX Titanium+ sequencer (Roche, Switzerland). DNA from one pellet from each strain was extracted using a PowerSoil DNA isolation kit (MO BIO, Carlsbad, CA) according to the manufacturer's instructions and then prepared for sequencing according to the manufacturer's instructions. A second pellet from each strain was used for resequencing at the same facility on the Ion Torrent PGM platform (Life Technologies), according to the manufacturer's instructions.

PCRs followed by Sanger dye terminator sequencing were performed to confirm variations or provide extra coverage for low- or no-coverage regions of the genomes. Primers were designed using Clone Manager 9 (Sci-Ed Software, Cary, NC) and ordered from Integrated DNA Technologies (Coralville, IA). See Table 1 for primers used. PCR was performed with DNA as the templates extracted with a DNeasy tissue kit (Qiagen, Valencia, CA) according to the manufacturer's instructions. Alternatively, cultures of bacteria were placed at −20°C overnight and then thawed and used as the template directly. Remaining reagents were *Ex Taq* (TaKaRa, Japan), HiFi HotStart (KAPA, Woburn, MA), or *Taq* (Qiagen) PCR kits. PCR reagent concentrations and thermal cycler protocols were according to the manufacturer's instructions. PCR products were run by electrophoresis on 1% agarose gels in Tris-acetate-EDTA (TAE) buffer with ethidium bromide. When necessary due to multiple bands, the band at the predicted size was physically cut out of the gel and extracted using a QIAquick gel extraction kit (Qiagen). PCR products were purified using a QIAquick PCR purification kit (Qiagen). Products were sent to Eton Bioscience (Research Triangle Park, NC) or ACGT, Inc. (Wheeling, IL), for dye terminator sequencing. Sequences were analyzed using FinchTV (Geospiza, Seattle, WA) and Geneious v6 (Biomatters Ltd., New Zealand) (22).

***In silico* assembly and sequence analysis.** The 454 reads were assembled using Geneious v6 software with the genome sequence of *A. vinelandii* strain DJ as a reference (accession number CP001157) (12). Single nucleotide polymorphisms (SNPs) and insertions/deletions (indels) were catalogued using Geneious with a 45% variant frequency cutoff. Ion Torrent data and Sanger sequencing reads were used primarily to confirm or reject variations detected in 454 data. *De novo* assembly was performed using Newbler (Roche, Switzerland) to confirm that there were no large rearrangements.

Bioreactor setup. Batch and chemostat experiments were performed using a Biostat Bplus 2-liter bioreactor (Sartorius, Germany) equipped with control units and sensors for pH (Mettler-Toledo, USA), temperature, dissolved oxygen (Mettler-Toledo), mass flow control (airflow), and agitation.

Chemostat experiments were performed in a culture volume of 700 ml; temperature was held at 30°C, and pH was allowed to vary freely. Compressed air was pumped in through a 0.2-μm-pore-size filter at a rate of 0.315 ± 0.05 liters per minute (lpm); the system was open to gas exchange with the atmosphere. Exhaust gases (O_2, N_2, CO_2, H_2, and Ar) were monitored and recorded redundantly in real time using in-line O_2/CO_2 EasyLine continuous gas analyzers, model EL3020 (ABB, Germany), and a Pfeiffer OmniStar quadrupole mass spectrometer. Culture turbidity was monitored and recorded in real time using an in-house device that continuously measures light transmittance through a section of glass tubing through which culture is recirculated (23). Arbitrary unit (AU) measurements from this device can be converted to optical density at 600 nm (OD_{600}) units with the following formula: OD_{600} units = 0.0177 × AU − 1.9583.

Media were prepared in 20-liter glass carboys as three separate solutions: 5 liters of salts in a 10-liter bottle, autoclaved 45 to 60 min; 12 liters of phosphates in the final 20-liter carboy, autoclaved 60 to 75 min; and 3 liters of sucrose and other remaining components, if any (iron and citrate in stepwise experiments), in a 3-liter bottle, filter sterilized. Media were then combined by transferring the salts and sucrose solutions into the final carboy using filtered air pressure. The final volume was placed on a scale, and the weight loss per unit of time was monitored and recorded continuously throughout the experiments.

For each experiment, the reactor, set to the appropriate temperature (30°C) and dissolved oxygen concentration (30%), was inoculated by injection of pregrown cells in a flask batch culture. When the culture reached exponential phase, the inflow of fresh medium and removal of excess culture volume were initiated. Steady state was achieved before starting any sampling.

System parameters were defined as follows: the dilution rate (D) is the value obtained after reaching equal feed and harvest flows that allow for obtaining a constant volume of culture in the reactor ($D = F/V$). Yield is defined as the ratio of product generated to limiting substrate (sucrose) consumed. Productivity is the value of product generated per limiting substrate consumed per unit of time.

Batch growth conditions were similar to chemostat culture setup, described above, except that the reactor volume was 1 liter, Burk medium contained 2.5 mg $FeSO_4 \cdot 7H_2O$ and 2.5 mg ferric citrate per liter, reactor cultures were initiated by inoculation to a density of $OD_{600} = 0.1$, and airflow through the reactor was set at 1 lpm at 1 atmosphere (atm). Dissolved oxygen was maintained above 30% by master control linked to the agitation speed between range limits of 300 to 1,000 rpm using a proportional-integral-derivative (PID) control system. Culture turbidity was monitored and recorded in real time using an in-house device, as in the chemostat culture setup. In all determinations of exhaust gas composition, the final concentrations were obtained by subtracting the amount of the compounds present in the air. Total compound mass was obtained by calculating the area under the production curves of H_2 and CO_2, and yields were calculated by dividing the overall mass of each gas produced by the mass of limiting substrate (sucrose) consumed. Biomass measurements were obtained as dry weights as described in "Sample Analysis" below.

Iron limitation evaluations. (i) Iron uptake analysis in batch culture. *A. vinelandii* CA and CA6 were tested for their iron uptake abilities: the strains were transferred on solid Mo-deficient medium containing

TABLE 1 Primers used

Location of 5′ end in strain DJ	Direction	Primer sequence	Purpose
1186882	Forward	5′-GTGCTGGCGAGATCGACGCTGTTC-3′	Resequence a low-coverage region
1187926	Reverse	5′-GCGGCGGCAATGGCGTGACTTA-3′	Resequence a low-coverage region
2866462	Forward	5′-GTAGGTATCGCTGGCCTGTTCCAA-3′	Resequence a low-coverage region
2866751	Reverse	5′-TCACCGGACTTTCAGCTCCCTCTTC-3′	Resequence a low-coverage region
3182590	Forward	5′-TGCGAACTACGCCAGTGACATT-3′	Confirm insertion in DJ
3182937	Reverse	5′-CGCCCTGTATTAGCCAGCAAAGAC-3′	Confirm insertion in DJ
2523005	Forward	5′-TGGTGGCGGCAGTAGTCGGAATC-3′	Confirm insertion in CA or CA6
2523341	Reverse	5′-GACACGGCGAAAGGCAACGCAT-3′	Confirm insertion in CA or CA6
5317895	Forward	5′-GGCGAGGCGGCGTTGATATTCT-3′	Resequence a low-coverage region
5318787	Reverse	5′-GGGAAACGGGTGCAGTTCCTAC-3′	Resequence a low-coverage region
496737	Forward	5′-GCGCGGTGCTTCCCGTCGTCGTGG-3′	Resequence a low-coverage region
497350	Reverse	5′-ACGGCGGCCCTTACCCGGCCACCT-3′	Resequence a low-coverage region
2866243	Forward	5′-CCGTCCGGCGAGACGGCTGTCGTA-3′	Resequence a low-coverage region
2867001	Reverse	5′-GGCGCTGCCCGAGCGGGAGAAACT-3′	Resequence a low-coverage region
3726483	Forward	5′-GCTGGCTGACCAGACTGACGATCA-3′	Resequence a low-coverage region
3727301	Reverse	5′-CCAAGGCGGCGGAACAAAGGAAAG-3′	Resequence a low-coverage region
5102727	Forward	5′-GCGCCGACGACCGGCTCCATGT-3′	Confirm 42-kbp deletion in CA6
5145496	Reverse	5′-CCGCCGCTGCGTGGCCTGTTCT-3′	Confirm 42-kbp deletion in CA6
5103533	Reverse	5′-ACCCGCCGGGCATTCGCGTAGG-3′	Confirm lack of CA6's 42-kbp deletion in CA
1107618	Forward	5′-GACTGGCAGCGGCGGCAGAAC-3′	Confirm deletion in CA
1107955	Reverse	5′-GCCTCGTCGGCGAACGGACTC-3′	Confirm deletion in CA
3868445	Forward	5′-CGAGGGTGTCGCCGTCGTTGA-3′	Confirm SNP in CA6
3868718	Reverse	5′-CGCCCAGTTGTTCGCCTGA-3′	Confirm SNP in CA6
5303255	Forward	5′-CGGTCTCCCGGCTGGACCCGATCA-3′	Sequence a no-coverage region
5304504	Reverse	5′-CCGGCGAACTGGCCGCGATGACCC-3′	Sequence a no-coverage region
2014002	Forward	5′-ACCGATTTCTCGCCGCTGCAATAG-3′	Sequence a no-coverage region
2014929	Reverse	5′-GCCCAGGACGAGTACATCGCAATA-3′	Sequence a no-coverage region
4415777	Forward	5′-CGAACGAGGCTTCGGCAAGGATT-3′	Sequence a no-coverage region
4416690	Reverse	5′-TACCTGGGCGGCAAGGCCGGGTAG-3′	Sequence a no-coverage region
4424706	Forward	5′-AGAAACAGCGGCACGTCCTCGATA-3′	Sequence a no-coverage region
4425701	Reverse	5′-CGAGCACGACATCAAGGTGGTCAT-3′	Sequence a no-coverage region
5124867	Forward	5′-CGGCTTGTCGGTGATGACCTT-3′	Confirm marker insertion in HS2's *hoxK*
5125741	Reverse	5′-CGGTATGGAGCGGGCATTTC-3′	Confirm marker insertion in HS2's *hoxK*
5125712	Forward	5′-ACGGTTTGGTTGATGCGAGTG-3′	Determine insertion location inside HS2's *hoxK*
5125544	Reverse	5′-GGGATCGCAGTGGTGAGTAAC-3′	Determine insertion location inside HS2's *hoxK*
4686350	Forward	5′-TCGCCAGACTCCTTGTTGAAA-3′	Confirm transposon insertion in CA
4687563	Reverse	5′-TGTAAGTGTGCCAGCAAAGTG-3′	Confirm transposon insertion in CA

fixed nitrogen and then cultured for use as inocula in liquid medium of the same composition as in similar molybdenum accumulation studies (24). Briefly, 200-ml cultures were grown to late log phase in 1-liter side-arm flasks containing $FeSO_4$-deficient medium supplemented with ammonia. The cells were collected by centrifugation and resuspended in fresh N-sufficient, $FeSO_4$-deficient medium. For the Fe uptake time course, $FeSO_4$ was added to a final concentration of 5 μM, and the culture was shaken vigorously at 30°C. At selected time intervals, 10-ml aliquots of the culture were withdrawn; the cells were pelleted by centrifugation, washed with Mo-free phosphate buffer (7 mM, pH 7.0), and resuspended in 1 ml of water. The iron content of the cell suspension was determined by the inductively coupled plasma atomic emission spectroscopy method by the North Carolina State University Analytical Laboratory. Each value is the average from three replicates for CA and four replicates for CA6.

(ii) Transient responses to iron additions in the chemostat. The medium used was nitrogen-free Burk as described above, containing 50 mg/liter $FeSO_4 \cdot 7H_2O$, autoclaved along with the 5 liters of salt solution. When the three component solutions were combined, a precipitate formed at the bottom of the carboy, where it was inaccessible to the feed tube; this served to enhance any observed effects of iron limitation. This medium was used for all three strains tested. Sucrose was the sole source of carbon and energy. Samples of each batch of medium were saved at −80°C for later analysis.

The dilution rate for these chemostat experiments was set to 0.038 h^{-1}. Once steady state was achieved, a pulse of one of the following was injected into the reactor: (i) 7 ml containing 1.4 g sucrose; (ii) sucrose as in i, plus 0.7 ml containing 1.75 mg each $FeSO_4 \cdot 7H_2O$ and ferric citrate; (iii) 7 ml containing 1.54 g ammonium acetate; or (iv) a combination of iii with i or ii. Adding citrate is an established method for maintaining iron in a soluble form over the length of a chemostat experiment (25, 26). No pulses were made until after at least four retention times had passed and steady state was reestablished. Retention time is the time required to replace one reactor volume of culture with fresh medium, 1/D; for example, at D = 0.038 h^{-1}, 700 ml pass through the system in approximately 26 h, one retention period.

Determination of yields by stepwise increases in concentration of the growth-limiting substrate. The medium used was nitrogen-free Burk, as described above, except it contained 5 mg $FeSO_4 \cdot 7H_2O$ and 0.5 g sodium citrate per liter, filter sterilized along with the sucrose in the 3-liter bottle. The citrate prevented the other components from precipitating, so everything remained in solution, as described previously (25). For tungstate-containing chemostats with CA6, sodium tungstate was added to a 1 mM final concentration. To increase sucrose concentrations, 3 liters of complete nitrogen-free Burk medium was assembled with enough extra sucrose to increase the concentration in the medium remaining in the 20-liter carboy to the desired values. The 3-liter volume of medium was

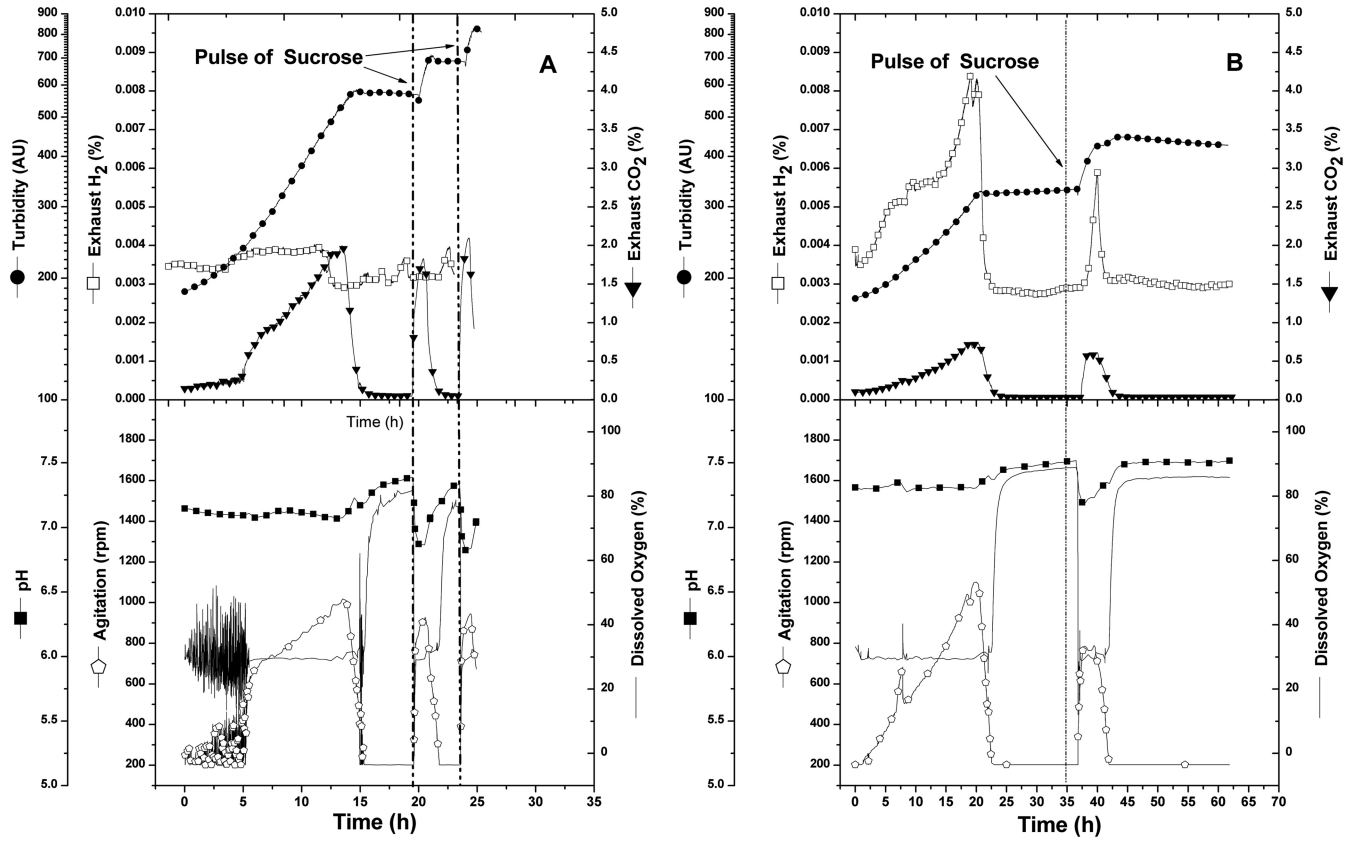

FIG 2 Batch culture experiments of *A. vinelandii* CA and CA6 strains growing in nitrogen-free Burk medium (1-lpm airflow, 30°C, 30% dissolved oxygen). Vertical dotted lines indicate pulses of additional substrate. (A) CA; (B) CA6.

filter sterilized and added to the 20-liter carboy using filtered air pressure. A sample of each batch of medium at each concentration was saved at −80°C for later analysis.

The dilution rate for these experiments was set to 0.066 h^{-1}. Once steady state was achieved, at least three samples were taken and analyzed before the sucrose concentration was changed. At least one retention period was allowed to pass between each sample; at $D = 0.066$ h^{-1}, 700 ml passed through the system in approximately 15 h.

Sample analysis. Each sample was spun down for 5 min at 10,000 rpm in an Eppendorf centrifuge 5417R (Eppendorf, USA), and then the supernatant and pellet were saved in separate tubes at −80°C for later analysis. OD_{600} was determined using an Ultrospec 1100 pro spectrophotometer. Dry weight was obtained by filtering a portion of sample using vacuum suction through a 0.2-μm-pore-size filter of known mass (mixed cellulose esters; EMD Millipore, Germany); the filter was then dried at 60 to 70°C for 1 to 7 days and reweighed until weight was constant to determine the dry weight of biomass per sample volume.

The initial and residual concentrations of sucrose were determined from samples of initial media and supernatants of reactor samples analyzed by a high-performance liquid chromatograph (Shimadzu, Japan) run under isocratic conditions at 65°C. The mobile phase was water at 0.5 ml/min, and the column was Supelcogel Ca (300 mm by 7.8 mm; Supelco Analytical, Bellefonte, PA, USA). The column was coupled to a refractive index detector. Absolute values were obtained by measuring known quantities of sucrose to generate a standard curve.

Statistics. The significance of differences between strains' iron uptake values was evaluated using Gosset's *t* test.

Nucleotide sequence accession numbers. Final annotated versions of the genomes of CA and CA6 were submitted to GenBank; accession numbers are CP005094 (CA) and CP005095 (CA6) (27).

RESULTS

Batch experiments confirmed CA6 hydrogen generation phenotype. *A. vinelandii* strain CA6 is able to fix nitrogen in the presence of tungstate (7) and also exhibits impaired molybdate uptake (9). A third phenotypic characteristic not previously evaluated is CA6's ability to generate molecular hydrogen. To confirm hydrogen generation capabilities, we performed batch cultures (using benchtop reactors) and compared the kinetic and yield parameters of CA and its offspring CA6 (Fig. 2 and Table 2). Under identical nitrogen-free culturing conditions, strain CA6 showed a reduced growth rate, reduced biomass yield, and increased amounts of hydrogen evolution compared to its parent. CA6 hydrogen generation reached 37.21 mmol hydrogen per mole of sucrose consumed, while CA's evolution was negligible. Also notable was how robust these activities were after carbon limitation in nitrogen-free medium: despite a 17.5-h starvation period, CA6 was able to resume growth and initiate hydrogen production following a pulse of sucrose (Fig. 2B). Table 2 provides the kinetic and yield values calculated for each strain under these conditions. The data show identical levels of CO_2 generation, demonstrating that sucrose was always the growth-limiting substrate and no products other than biomass, CO_2, and molecular hydrogen were produced. Furthermore, CA6's phenotype has a clear energetic impact, as shown by the reduced biomass yield and specific growth rate.

Whole genomic comparison of *A. vinelandii* CA and CA6. The genomes of strains CA and CA6 were sequenced and com-

TABLE 2 Kinetic and yield parameters obtained from batch culture experiments of *A. vinelandii* strains CA and CA6 growing in nitrogen-free Burk medium[b]

		Hydrogen and CO_2 yields									
		Biomass yield ($Y_{X/S}$)		End of growth phase, 20 g/liter sucrose (limiting growth substrate)				Stationary phase pulse, 5 g/liter sucrose (limiting growth substrate)			
Strain	μ^a (h^{-1})	mg X/g S	C-mol X/mol S	g CO_2/g S	mol CO_2/mol S	mol CO_2/mmol H_2	mmol H_2/mol S	g CO_2/g S	mol CO_2/mol S	mol CO_2/mmol H_2	mmol H_2/mol S
CA	0.29	41.46	0.55	0.687	5.34	>53	<0.1	0.48	3.8	>38	<0.1
CA6	0.15	24.5	0.324	0.66	4.95	0.13	37.21	0.454	3.53	0.52	6.7

[a] Maximum specific growth rate.
[b] Conditions are 1-lpm airflow, 30°C, 30% dissolved oxygen. X, dry-weight biomass; S, sucrose.

pared to the *A. vinelandii* reference genome (12) to determine the genetic polymorphisms responsible for the physiological differences (slower growth, impaired molybdate uptake, hydrogen evolution, and tolerance to tungstate) and to facilitate functional associations of genotype with phenotype.

Two techniques were used: 454 pyrosequencing and ion torrent sequencing provided 63- to 64-fold coverage for each genome, mapping to a depth between 0 and 228 reads per position. More sequencing details can be found in Table S1 in the supplemental material. Gaps and shallow areas were resequenced using PCR and dye terminator sequencing.

Mapping reads from *A. vinelandii* CA to the genome sequence of *A. vinelandii* strain DJ, a high-frequency transforming variant of CA whose genome had previously been published (12), revealed a number of small variations, both single nucleotide polymorphisms (SNPs) and insertions/deletions (indels), between the two strains (see Table S2 in the supplemental material), but overall the genomes displayed greater than 99.9% pairwise identity.

The comparison of reads from strain CA6 with DJ's genome revealed a conspicuously large deletion in the CA6 genome, encompassing 42 whole or partial open reading frames. Because of this deletion, identity between CA6 and DJ is only 99.2%. Figure 3 shows an atlas with the locations of all mutations in CA6, and Table S2 lists other minor variations between strains.

The large deletion in CA6 eliminates several operons from the strain, which may contribute to CA6's mutant phenotypes. These operons include the *hox* operon, encoding the membrane-bound uptake hydrogenase, with its accessory protein-encoding genes in the *hyp* operon (20, 28, 29). Also missing are most of the iron transporter-encoding *fhu* operon, the well-characterized molybdate transporter-encoding *mod1* operon, and a putative molybdate transporter-encoding *mod3* operon (Fig. 4) (12, 30–32).

Iron uptake analysis. The deletion of the *fhu* iron transporter in CA6 suggests a defect in iron uptake. To confirm impairment, we inoculated iron-depleted CA and CA6 cells into a batch culture of iron-replete medium and measured iron accumulation over time. At 60- and 120-min time points, CA6 contained significantly less intracellular iron than its parent CA (Table 3).

Transient response experiments confirm iron uptake limitation in CA6. The CA6 phenotypes of slower growth, tolerance to tungstate, and impaired molybdate uptake had previously been observed (9), and the batch cultures described above also demonstrate hydrogen evolution capabilities. Therefore, to determine whether the newly discovered deletion of the iron transporter-encoding *fhu* operon in CA6 could result in iron-limiting growth, and whether such a phenotype could influence hydrogen production, chemostat experiments were performed comparing *A. vinelandii* strains CA, CA6, and HS2 (a strain in which the hydrogenase gene *hoxK* was knocked out [20]). The strain HS2 was included in this study since it retains the *fhu* operon and other metal transporters missing in CA6, so HS2 cultures should not encounter limiting levels of iron as readily as CA6. After achieving steady-state conditions with each strain in a low-iron, carbon-limiting, nitrogen-free Burk medium, pulses of sucrose and iron or sucrose alone were tested. This strategy allows for identification of limiting growth factors and has been utilized for medium optimization (33, 34). If the tested element acts as a growth-limiting factor, the products of the culture should increase transiently and then recover to steady-state levels after the washout. As expected, the addition of iron with sucrose did not affect the amount of biomass, hydrogen, or CO_2 generated by CA or HS2 from the additional carbon, whereas the increase in these products approximately doubled when iron was added with sucrose to steady-state CA6 cultures (data not shown).

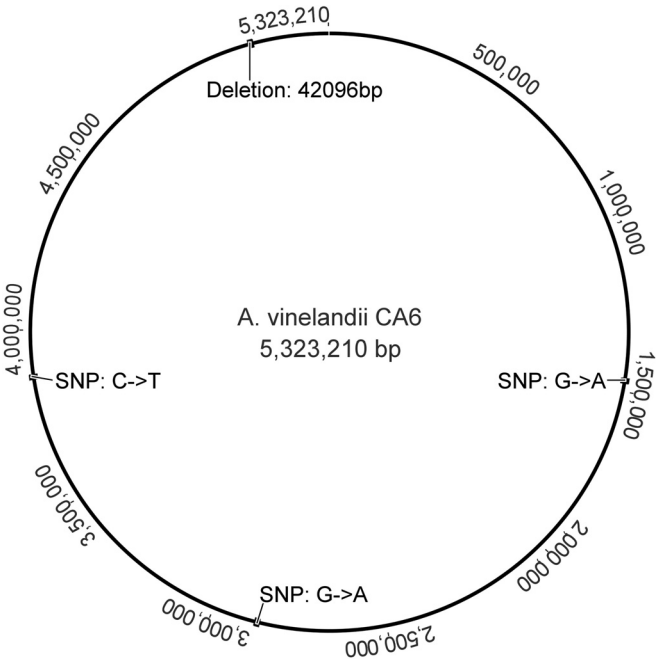

FIG 3 Mutations in the genome of *A. vinelandii* CA6. Numbers on the outside show base numbers of genome locations in CA6. Image produced using Geneious.

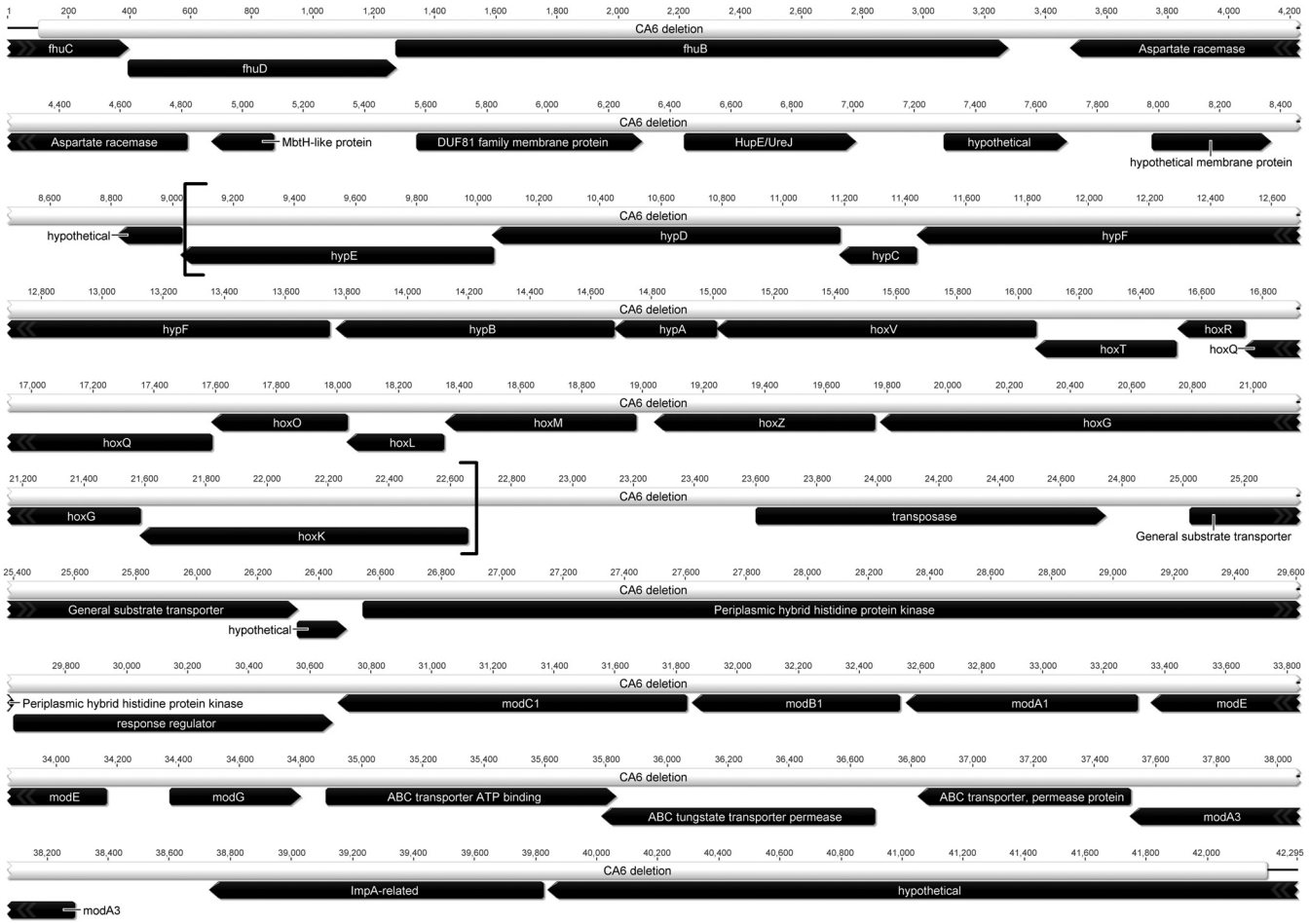

FIG 4 Schematic representation of a section of CA's genome, moving from the top left corner to the bottom right, with annotations marking the CA6 42-kbp deletion (white) and all genes included (black). Arrows indicate strand orientation of each gene. Brackets indicate genes involved in uptake hydrogenase. Image produced using Geneious.

In addition to regulation of the alternative nitrogenases in the presence of heterometals, wild-type *A. vinelandii* represses nitrogen fixation in the presence of fixed nitrogen (21, 35, 36). *A. vinelandii* CA6 lacks Mo-induced repression of alternative nitrogenases; to discover if it also lacks regulation of nitrogenase activity in the presence of fixed nitrogen, steady-state cultures of CA6 and HS2 were tested by pulsing nitrogen in the form of ammonium acetate, by itself or in combination with sucrose or sucrose and iron. All pulses produced an immediate cessation of hydrogen production in both strains, and hydrogen production gradually resumed as the ammonium washed out or was consumed (Fig. 5).

TABLE 3 Iron accumulated over time by *A. vinelandii* strains CA and CA6[a]

Time (min)	Iron accumulation (pg/ml) by strain		
	CA	CA6	*P* value
0	60.6	41.0	0.46
5	741.3	624.7	0.54
60	791.4	320.9	0.005[b]
120	704.2	280.7	0.007[b]
1200	162.9	72.1	0.16

[a] All values are averages from three replicates for CA and four replicates for CA6. *P* value indicates significance of Gosset's *t* test comparing values for the two strains.
[b] $P < 0.05$.

Determination of yields by stepwise increases in concentration of the growth-limiting substrate using chemostats. We conducted a series of tightly controlled aerobic, carbon-limiting chemostat culture experiments in iron-sufficient and nitrogen-free medium. By varying the concentration of sucrose in the medium, we established stepwise steady states and compared the biomass (dry weight), CO_2, and hydrogen production capabilities of *A. vinelandii* strains CA, CA6, and HS2 at each steady-state sucrose feed rate. Steady-state values of dry weight, hydrogen, and carbon dioxide over sucrose consumed were plotted, and the yields were calculated from the slope of the resulting best-fit lines. Figure 6 shows graphs of product over substrate for biomass, hydrogen, and CO_2, and Table 4 provides calculated yields and productivity values for the three tested strains. Notably, under the conditions tested, CA6 and HS2 are nearly identical in yields for all three products, and each produces almost 100-fold more hydrogen per gram of substrate than CA and slightly less (not statistically significant) biomass and CO_2 (Table 4).

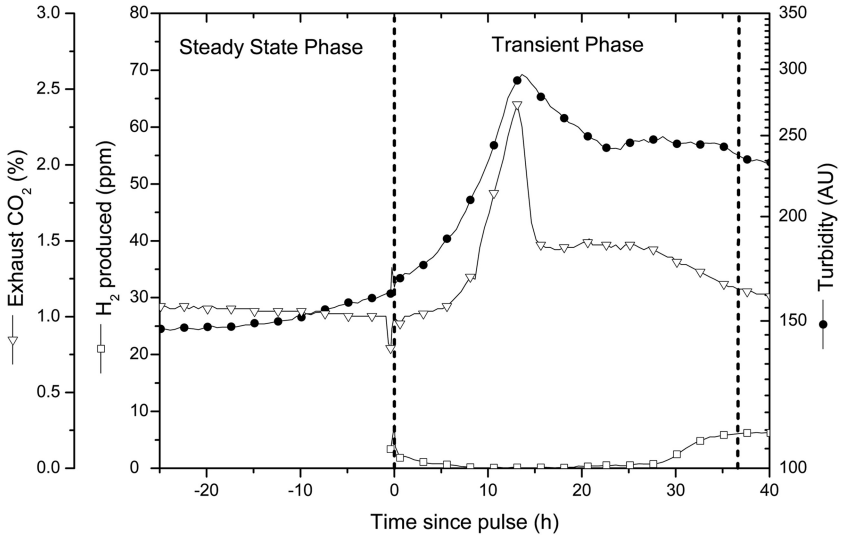

FIG 5 Transient response to nitrogen pulses applied to aerobic, carbon-limited, steady-state chemostat cultures ($D = 0.033\ h^{-1}$) of *A. vinelandii* CA6 growing at 30°C in nitrogen-free Burk medium. The leftmost vertical dashed line indicates the pulse time; to the left of it the culture is in steady state, and to the right a transient phase occurs as the cells respond to the addition of the limiting component (1.54 g ammonium acetate, 1.4 g sucrose, and 1.75 mg $FeSO_4 \cdot 7H_2O$). To the right of the rightmost vertical dashed line, a steady state resumes after pulse contents are consumed or washed out.

Enhancement of CA6 hydrogen production by the addition of tungstate. When molybdate is present in nitrogen-free medium, CA preferentially uses its primary nitrogenase, but CA6 produces both the primary and iron-only nitrogenases under these conditions, resulting in its tungstate tolerance phenotype (9). Considering that the iron-only nitrogenase is less efficient (a higher proportion of its electron flux goes to reducing protons instead of N_2), we expected that tungstate would poison CA6's primary nitrogenase, forcing it to rely on the alternative nitrogenase and increasing hydrogen yield as a result. We repeated the stepwise chemostat experiment with CA6 with 1 mM tungstate and no added molybdate in the medium (Fig. 6 and Table 4). This experiment is possible only with CA6, not the other strains, because of tungsten's nitrogenase-poisoning effect (7, 8). Compared to CA6 in the absence of tungstate, tungsten-grown CA6's hydrogen yield increased about 4.5-fold, while biomass yield decreased about 30% and CO_2 about 10%.

DISCUSSION

The primary genetic change that generates the phenotypic differences between *A. vinelandii* CA and its offspring CA6 is a 42-kbp deletion, which removes a number of genes, including genes encoding metal transporters and the uptake hydrogenase, and allows for coexpression of the primary and alternative nitrogenases. The origin of CA6's large deletion is a curiosity. The strain was isolated through directed evolution when the parent strain was exposed to tungstate (7), a straightforward and common methodology (7, 37, 38), but this manner of large deletion has not previously been described. The mechanism of deletion and the precise mechanism of tolerance to tungstate invite further study.

A. vinelandii CA6's known mutant phenotypes are impaired growth in some conditions, impaired molybdate uptake, and tolerance to tungstate via derepression of alternative nitrogenases (7, 9). Other phenotypes characterized in this study are hydrogen production (enhanced by the presence of tungstate) and impaired

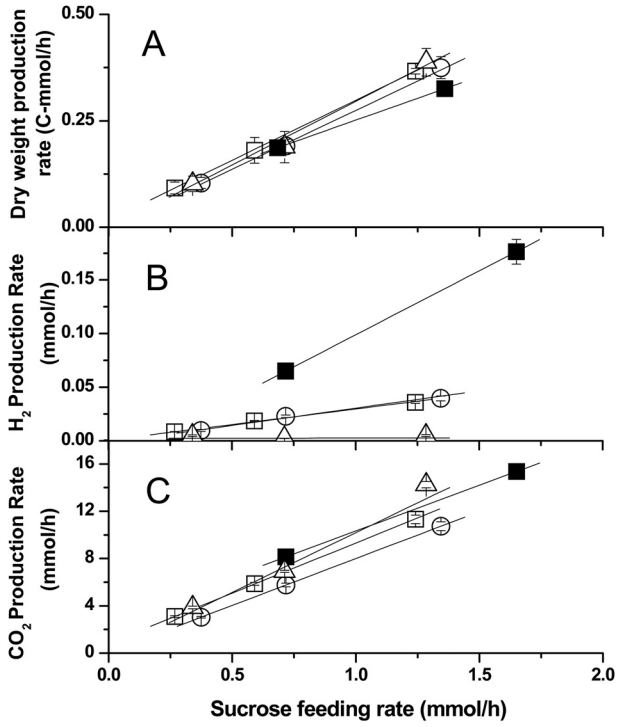

FIG 6 Generation rates of biomass (dry weight), CO_2, and hydrogen in response to increases in sucrose feeding rates of *A. vinelandii* strains growing in chemostat culture ($D = 0.066\ h^{-1}$) at 30°C in iron-sufficient, nitrogen-free Burk medium. Triangles (△) give values for strain CA, circles (○) for HS2, empty squares (□) for CA6, and filled squares (■) for CA6 plus tungsten. Error bars (present for all points) indicate standard deviations. Yield values given in Table 4 were obtained for each strain by calculating the slope of the best-fit line for these points for each strain. (A) Dry weight values, in carbon moles (standardized by moles of carbon); (B) values for hydrogen, given as hydrogen produced, i.e., total hydrogen minus environmental hydrogen; (C) values for CO_2, given as CO_2 produced, i.e., total CO_2 minus environmental CO_2.

TABLE 4 Kinetic and yield parameters from stepwise chemostat experiments, calculated from slopes of lines in Fig. 6

Parameter	Value by strain			
	CA	CA6	HS2	CA6 plus tungsten
Dilution rate (h^{-1})	0.066	0.066	0.066	0.066
Biomass yield (mg dry wt g^{-1} substrate)	23.58	21.72	21.63	15.78
Hydrogen yield (μg H_2 g^{-1} substrate)	1.93	164.18	178.21	697.64
CO_2 yield (g CO_2 g^{-1} substrate)	1.43	1.08	1.02	0.99
H_2 productivity (μg H_2 g^{-1} substrate h^{-1})	0.13	10.84	11.76	46.04
CO_2 productivity (g CO_2 g^{-1} substrate h^{-1})	0.09	0.07	0.07	0.07
Biomass productivity (mg dry wt g^{-1} substrate h^{-1})	1.56	1.43	1.43	1.04

iron uptake. It is likely that all these phenotypes are due to the large chromosomic deletion in CA6 (Fig. 4).

Two operons lost in the deletion are related to molybdate transport: the *mod1* and putative *mod3* operons. Previous work to elucidate the ability of CA6 to grow in the presence of tungstate evaluated the *mod1* operon; specifically, the regulatory gene *modE* was knocked out, resulting in lower molybdate accumulation at high medium concentrations (9, 30). Since ModE and ModB are also involved in molybdate-induced repression of the alternative nitrogenases (31, 39), their deletion partially explained the CA6 phenotypes. However, the deletion does not completely abolish molybdate uptake, possibly due to the *mod2* operon located elsewhere in the genome (12). Premakumar et al. reasoned that the mutant's slower growth than that of its parent is due to its production and use of two nitrogenase isoenzymes simultaneously, one less efficient than the other (9). Further experimentation is needed to elucidate the *mod* genes' precise roles in regulation and physiology.

The discovery of the large deletion in CA6 unveiled two other changes that led to the observation of new phenotypes. First, a possible impairment of iron transport due to the deletion of the *fhu* operon: we explored this phenotype functionally and determined the conditions required to avoid iron limitation when cultivating CA6. The second phenotype was hydrogen evolution by CA6: it corresponded to the lack of hydrogenase genes (*hox* and *hyp*) within the deleted region in CA6. The products of these operons are responsible for the oxidation of hydrogen gas (20, 28, 40), and without these enzymes, the hydrogen that *A. vinelandii*'s nitrogenases generate as a by-product escapes the cell. Additions of ammonium and iron also confirmed the nitrogenases' role in *Azotobacter* hydrogen generation since the presence of ammonium inhibited both nitrogenase activity and hydrogen production.

Eliminating our mutant's iron limitation using an iron-sufficient, nitrogen-free medium allowed for a comparison of the hydrogen-producing capabilities of CA, CA6, and HS2 (a single-gene [*hoxK*] knockout strain derived from CA [15]). The findings reveal that both mutants (CA6 and HS2) produce similar amounts of hydrogen under these conditions; the deficiency of a single gene (*hoxK*) was sufficient to replicate the hydrogen evolution and impaired-growth phenotypes of CA6 under the conditions tested (Table 4). Surprisingly, despite CA6 coexpressing both the primary and less efficient iron-only nitrogenases (9), we observed no difference in hydrogen produced from CA6 compared with that from strain HS2, which produces only the primary nitrogenase in the presence of molybdate. Additionally, the unique capability of CA6 to grow in the presence of tungstate allowed us to test the role of the iron nitrogenase in hydrogen evolution and demonstrate that increased hydrogen yields can be obtained using CA6. Under these conditions, when only the iron-only nitrogenase could fix nitrogen, the cells produced larger amounts of molecular hydrogen, generating about 4.5-fold more hydrogen than with tungstate absent (Table 4). This is in line with previous observations in several nitrogen-fixing species (4, 10, 15, 41–44). Another interesting possibility is that tungsten replaces Mo in the central dinitrogenase cofactor, rendering the enzyme capable only of proton reduction to H_2 (45). In such a scenario, the

TABLE 5 Comparison of CA6 with other hydrogen-producing organisms

Organism	Reactor type[a]	Temp (°C)	Substrate	Substrate concn (g/liter)	Hydrogen yield (mol H_2/mol glucose, hexose equivalent)	Hydrogen production rate (liter H_2/liter culture/day)	Reference or source
Azotobacter vinelandii CA6	CSTR	30	Sucrose	10	0.06	0.03	This study
CA6 plus tungsten	CSTR	30	Sucrose	10	0.24	0.15	This study
Escherichia coli WDHL	Batch	37	Glucose	15	0.30	0.45	47
Clostridium butyricum CWBI1009	Batch	30	Glucose	5	1.70	3.02	48
Clostridium tyrobutyricum JM1	CSTR	37	Glucose	5	1.81	7.21	49
Thermotoga neapolitana DSM 4359	Batch	80	Glucose	7.5	1.84	6.05	50
Ethanoligenens harbinense YUAN-3	CSTR	35	Glucose	10	1.93	19.6	51
Clostridium butyricum W5	Batch	37	Glucose	3	2.09	0.41	52
Enterobacter aerogenes W23 plus *Candida maltosa* HY-35	Batch	35	Glucose	5	2.19	6.27	53
Enterobacter aerogenes IAM 1183	Batch	37	Galactose	10	2.82	6.96	54
Thermotoga neapolitana DSM 4359	CSABR	75	Xylose	5	3.36	2.66	55
Thermotoga neapolitana DSM 4359	Batch	85	Glucose	2.5	3.75	0.54	56

[a] CSTR, continuous stirred tank reactor; CSABR, continuously stirred anaerobic bioreactor.

product of *nif* genes would not fix nitrogen, only produce hydrogen.

A. vinelandii has long been recognized as a robust nitrogen-fixing species, and strain CA6 represents an unusual type of hydrogen-producing microbe. It is an obligate aerobe, unlike strains that produce hydrogen through fermentation, and also a chemotroph, deriving its energy from organic substrates rather than light. Such a biohydrogen producer has the potential to fill a special niche in the range of hydrogen production technologies in which these characteristics are desirable. CA6's hydrogen yield from sucrose is about 5- to 60-fold lower than other candidate biohydrogen systems (mostly fermentative), though only up to 16-fold lower when tungstate was present (Table 5) (46). It may be better suited as a model for aerobic hydrogen production than for industrial purposes, but modifications to its genome and culture conditions may lead to dramatic improvements.

In conclusion, we have characterized CA6, a mutant strain of *A. vinelandii* lacking a number of important genes, which produces significant amounts of hydrogen. Further study is needed to fully characterize and optimize its hydrogen-producing capabilities.

ACKNOWLEDGMENTS

Thanks to Robert L. Robson for strain HS2.

J.N. was the recipient of a 3-year National Science Foundation Graduate Research Fellowship. This project was supported by the North Carolina State University Department of Microbiology (now Plant and Microbial Biology). The University of North Carolina—Chapel Hill Core facility is supported by grant number NIH P30 DK34987.

REFERENCES

1. **Bishop PE, Premakumar R.** 1992. Alternative nitrogen fixation systems, p 737–762. *In* Stacey G, Burns R, Evans H (ed), Biological nitrogen fixation. Chapman & Hall, New York, NY.
2. **Joerger RD, Jacobson MR, Premakumar R, Wolfinger ED, Bishop PE.** 1989. Nucleotide sequence and mutational analysis of the structural genes (*anfHDGK*) for the second alternative nitrogenase from *Azotobacter vinelandii*. J Bacteriol **171:**1075–1086.
3. **Luque F, Pau RN.** 1991. Transcriptional regulation by metals of structural genes for *Azotobacter vinelandii* nitrogenases. Mol Gen Genet **227:**481–487. http://dx.doi.org/10.1007/BF00273941.
4. **Pau RN, Eldridge ME, Lowe DJ, Mitchenall LA, Eady RR.** 1993. Molybdenum-independent nitrogenases of *Azotobacter vinelandii*: a functional species of alternative nitrogenase-3 isolated from a molybdenum-tolerant strain contains an iron-molybdenum cofactor. Biochem J **293:**101–107.
5. **Jacobson M, Premakumar R, Bishop P.** 1986. Transcriptional regulation of nitrogen-fixation by molybdenum in *Azotobacter vinelandii*. J Bacteriol **167:**480–486.
6. **Jacobitz S, Bishop PE.** 1992. Regulation of nitrogenase-2 in *Azotobacter vinelandii* by ammonium, molybdenum, and vanadium. J Bacteriol **174:**3884–3888.
7. **Bishop PE, Jarlenski DM, Hetherington DR.** 1980. Evidence for an alternative nitrogen fixation system in *Azotobacter vinelandii*. Proc Natl Acad Sci U S A **77:**7342–7346. http://dx.doi.org/10.1073/pnas.77.12.7342.
8. **Benemann JR, Smith GM, Kostel PJ, McKenna CE.** 1973. Tungsten incorporation into *Azotobacter vinelandii* nitrogenase. FEBS Lett **29:**219–221. http://dx.doi.org/10.1016/0014-5793(73)80023-7.
9. **Premakumar R, Jacobitz S, Ricke SC, Bishop PE.** 1996. Phenotypic characterization of a tungsten-tolerant mutant of *Azotobacter vinelandii*. J Bacteriol **178:**691–696.
10. **Krahn E, Schneider K, Müller A.** 1996. Comparative characterization of H_2 production by the conventional Mo nitrogenase and the alternative "iron-only" nitrogenase of *Rhodobacter capsulatus hup*$^-$ mutants. Appl Microbiol Biotechnol **46:**285–290. http://dx.doi.org/10.1007/s002530050818.
11. **Yates MG, Campbell FO.** 1989. The effect of nutrient limitation on the competition between an H_2-uptake hydrogenase positive (Hup$^+$) recombinant strain of *Azotobacter chroococcum* and the Hup$^-$ mutant parent in mixed populations. J Gen Microbiol **135:**221–226.
12. **Setubal JC, dos Santos P, Goldman BS, Ertesvag H, Espin G, Rubio LM, Valla S, Almeida NF, Balasubramanian D, Cromes L, Curatti L, Du Z, Godsy E, Goodner B, Hellner-Burris K, Hernandez JA, Houmiel K, Imperial J, Kennedy C, Larson TJ, Latreille P, Ligon LS, Lu J, Maerk M, Miller NM, Norton S, O'Carroll IP, Paulsen I, Raulfs EC, Roemer R, Rosser J, Segura D, Slater S, Stricklin SL, Studholme DJ, Sun J, Viana CJ, Wallin E, Wang B, Wheeler C, Zhu H, Dean DR, Dixon R, Wood D.** 2009. Genome sequence of *Azotobacter vinelandii*, an obligate aerobe specialized to support diverse anaerobic metabolic processes. J Bacteriol **191:**4534–4545. http://dx.doi.org/10.1128/JB.00504-09.
13. **Kow YW, Burris RH.** 1984. Purification and properties of membrane-bound hydrogenase from *Azotobacter vinelandii*. J Bacteriol **159:**564–569.
14. **Seefeldt LC, Arp DJ.** 1986. Purification to homogeneity of *Azotobacter vinelandii* hydrogenase: a nickel and iron containing αβ dimer. Biochimie **68:**25–34. http://dx.doi.org/10.1016/S0300-9084(86)81064-1.
15. **Bishop PE, Hawkins ME, Eady RR.** 1986. Nitrogen fixation in molybdenum-deficient continuous culture by a strain of *Azotobacter vinelandii* carrying a deletion of the structural genes for nitrogenase (*nifHDK*). Biochem J **238:**437–442.
16. **Benemann J.** 1996. Hydrogen biotechnology: progress and prospects. Nat Biotechnol **14:**1101–1103. http://dx.doi.org/10.1038/nbt0996-1101.
17. **Gregoire-Padró CE.** 1998. Hydrogen, the once and future fuel. Energy Fuels **12:**1–2.
18. **Mudhoo A, Forster-Carneiro T, Sánchez A.** 2011. Biohydrogen production and bioprocess enhancement: a review. Crit Rev Biotechnol **31:**250–263. http://dx.doi.org/10.3109/07388551.2010.525497.
19. **Bush JA, Wilson PW.** 1959. A non-gummy chromogenic strain of *Azotobacter vinelandii*. Nature **184:**381–381. http://dx.doi.org/10.1038/184381a0.
20. **Menon AL, Mortenson LE, Robson RL.** 1992. Nucleotide sequences and genetic analysis of hydrogen oxidation (*hox*) genes in *Azotobacter vinelandii*. J Bacteriol **174:**4549–4557.
21. **Strandberg GW, Wilson PW.** 1968. Formation of the nitrogen-fixing enzyme system in *Azotobacter vinelandii*. Can J Microbiol **14:**25–31. http://dx.doi.org/10.1139/m68-005.
22. **Kearse M, Moir R, Wilson A, Stones-Havas S, Cheung M, Sturrock S, Buxton S, Cooper A, Markowitz S, Duran C, Thierer T, Ashton B, Meintjes P, Drummond A.** 2012. Geneious basic: an integrated and extendable desktop software platform for the organization and analysis of sequence data. Bioinformatics **28:**1647–1649. http://dx.doi.org/10.1093/bioinformatics/bts199.
23. **Navarro-Herrero JL, Pico-Marco J, Bruno-Barcena JM, Valles-Albentosa S, Pico-Marco E.** December 2005. On-line method and equipment for detecting, determining the evolution and quantifying a microbial biomass and other substances that absorb light along the spectrum during the development of biotechnological processes. US patent 6,975,403.
24. **Pienkos PT, Brill WJ.** 1981. Molybdenum accumulation and storage in *Klebsiella pneumoniae* and *Azotobacter vinelandii*. J Bacteriol **145:**743–751.
25. **Kleiner D.** 1975. Ammonium uptake by nitrogen fixing bacteria. Arch Microbiol **104:**163–169. http://dx.doi.org/10.1007/BF00447319.
26. **Annison G, Couperwhite I.** 1986. Influence of calcium on alginate production and composition in continuous cultures of *Azotobacter vinelandii*. Appl Microbiol Biotechnol **25:**55–61.
27. **Noar JD, Bruno-Bárcena JM.** 2013. Complete genome sequences of *Azotobacter vinelandii* wild-type strain CA and tungsten-tolerant mutant strain CA6. Genome Announc **1:**e001313-13. http://dx.doi.org/10.1128/genomeA.00313-13.
28. **Chen JC, Mortenson LE.** 1992. Identification of six open reading frames from a region of the *Azotobacter vinelandii* genome likely involved in dihydrogen metabolism. Biochim Biophys Acta **1131:**199–202. http://dx.doi.org/10.1016/0167-4781(92)90077-D.
29. **Garg RP, Menon AL, Jacobs K, Robson RM, Robson RL.** 1994. The *hypE* gene completes the gene cluster for H_2-oxidation in *Azotobacter vinelandii*. J Mol Biol **236:**390–396. http://dx.doi.org/10.1006/jmbi.1994.1149.
30. **Mouncey NJ, Mitchenall LA, Pau RN.** 1995. Mutational analysis of genes of the *mod* locus involved in molybdenum transport, homeostasis, and processing in *Azotobacter vinelandii*. J Bacteriol **177:**5294–5302.
31. **Luque F, Mitchenall LA, Chapman M, Christine R, Pau RN.** 1993. Characterization of genes involved in molybdenum transport in *Azotobac-*

ter vinelandii. Mol Microbiol **7:**447–459. http://dx.doi.org/10.1111/j.1365-2958.1993.tb01136.x.
32. **Mouncey NJ, Mitchenall LA, Pau RN.** 1996. The *modE* gene product mediates molybdenum-dependent expression of genes for the high-affinity molybdate transporter and *modG* in *Azotobacter vinelandii*. Microbiology **142:**1997–2004. http://dx.doi.org/10.1099/13500872-142-8-1997.
33. **Mateles RI, Battat E.** 1974. Continuous culture used for media optimization. Appl Microbiol **28:**901–905.
34. **Kuhn H, Friederich U, Fiechter A.** 1979. Defined minimal medium for a thermophilic *Bacillus* sp. developed by a chemostat pulse and shift technique. Eur J Appl Microbiol Biotechnol **6:**341–349. http://dx.doi.org/10.1007/BF00499164.
35. **Bühler T, Sann R, Monter U, Dingler C, Kuhla J, Oelze J.** 1987. Control of dinitrogen fixation in ammonium-assimilating cultures of *Azotobacter vinelandii*. Arch Microbiol **148:**247–251. http://dx.doi.org/10.1007/BF00414820.
36. **Bühler T, Monter U, Sann R, Kuhla J, Dingler C, Oelze J.** 1987. Control of respiration and growth yield in ammonium-assimilating cultures of *Azotobacter vinelandii*. Arch Microbiol **148:**242–246. http://dx.doi.org/10.1007/BF00414819.
37. **Kajii Y, Kobayashi M, Takahashi T, Onodera K.** 1994. A novel type of mutant of *Azotobacter vinelandii* that fixed nitrogen in the presence of tungsten. Biosci Biotechnol Biochem **58:**1179–1180. http://dx.doi.org/10.1271/bbb.58.1179.
38. **Riddle GD, Simonson JG, Hales BJ, Braymer HD.** 1982. Nitrogen fixation system of tungsten-resistant mutants of *Azotobacter vinelandii*. J Bacteriol **152:**72–80.
39. **Premakumar R, Pau RN, Mitchenall LA, Easo M, Bishop PE.** 1998. Regulation of the transcriptional activators AnfA and VnfA by metals and ammonium in *Azotobacter vinelandii*. FEMS Microbiol Lett **164:**63–68. http://dx.doi.org/10.1111/j.1574-6968.1998.tb13068.x.
40. **Chen JC, Mortenson LE, Seefeldt LC.** 1995. Analysis of a gene region required for dihydrogen oxidation in *Azotobacter vinelandii*. Curr Microbiol **30:**351–355. http://dx.doi.org/10.1007/BF00369862.
41. **Eady R, Smith B, Postgate J, Cook K.** 1972. Nitrogenase of *Klebsiella pneumoniae*—purification and properties of component proteins. Biochem J **128:**655–675.
42. **Chisnell JR, Premakumar R, Bishop PE.** 1988. Purification of a second alternative nitrogenase from a *nifHDK* deletion strain of *Azotobacter vinelandii*. J Bacteriol **170:**27–33.
43. **Schneider K, Gollan U, Selsemeier-Voigt S, Plass W, Muffler A.** 1994. Rapid purification of the protein components of a highly active "iron only" nitrogenase. Naturwissenschaften **81:**405–408. http://dx.doi.org/10.1007/BF01132694.
44. **Schneider K, Gollan U, Dröttboom M, Selsemeier-Voigt S, Müller A.** 1997. Comparative biochemical characterization of the iron-only nitrogenase and the molybdenum nitrogenase from *Rhodobacter capsulatus*. Eur J Biochem **244:**789–800. http://dx.doi.org/10.1111/j.1432-1033.1997.t01-1-00789.x.
45. **Siemann S, Schneider K, Oley M, Müller A.** 2003. Characterization of a tungsten-substituted nitrogenase isolated from *Rhodobacter capsulatus*. Biochemistry **42:**3846–3857. http://dx.doi.org/10.1021/bi0270790.
46. **Elsharnouby O, Hafez H, Nakhla G, El Naggar MH.** 2013. A critical literature review on biohydrogen production by pure cultures. Int J Hydrog Energy **38:**4945–4966. http://dx.doi.org/10.1016/j.ijhydene.2013.02.032.
47. **Rosales-Colunga LM, Razo-Flores E, De León Rodríguez A.** 2012. Fermentation of lactose and its constituent sugars by *Escherichia coli* WDHL: impact on hydrogen production. Bioresour Technol **111:**180–184. http://dx.doi.org/10.1016/j.biortech.2012.01.175.
48. **Masset J, Hiligsmann S, Hamilton C, Beckers L, Franck F, Thonart P.** 2010. Effect of pH on glucose and starch fermentation in batch and sequenced-batch mode with a recently isolated strain of hydrogen-producing *Clostridium butyricum* CWBI1009. Int J Hydrog Energy **35:**3371–3378. http://dx.doi.org/10.1016/j.ijhydene.2010.01.061.
49. **Jo JH, Lee DS, Park D, Park JM.** 2008. Biological hydrogen production by immobilized cells of *Clostridium tyrobutyricum* JM1 isolated from a food waste treatment process. Bioresour Technol **99:**6666–6672. http://dx.doi.org/10.1016/j.biortech.2007.11.067.
50. **Nguyen TAD, Pyo Kim J, Sun Kim M, Kwan Oh Y, Sim SJ.** 2008. Optimization of hydrogen production by hyperthermophilic eubacteria, *Thermotoga maritima* and *Thermotoga neapolitana* in batch fermentation. Int J Hydrog Energy **33:**1483–1488. http://dx.doi.org/10.1016/j.ijhydene.2007.09.033.
51. **Xing D, Ren N, Wang A, Li Q, Feng Y, Ma F.** 2008. Continuous hydrogen production of auto-aggregative *Ethanoligenens harbinense* YUAN-3 under non-sterile condition. Int J Hydrog Energy **33:**1489–1495. http://dx.doi.org/10.1016/j.ijhydene.2007.09.038.
52. **Seppälä JJ, Puhakka JA, Yli-Harja O, Karp MT, Santala V.** 2011. Fermentative hydrogen production by *Clostridium butyricum* and *Escherichia coli* in pure and cocultures. Int J Hydrog Energy **36:**10701–10708. http://dx.doi.org/10.1016/j.ijhydene.2011.05.189.
53. **Lu W, Wen J, Chen Y, Sun B, Jia X, Liu M, Caiyin Q.** 2007. Synergistic effect of *Candida maltosa* HY-35 and *Enterobacter aerogenes* W-23 on hydrogen production. Int J Hydrog Energy **32:**1059–1066. http://dx.doi.org/10.1016/j.ijhydene.2006.07.010.
54. **Ren Y, Wang J, Liu Z, Ren Y, Li G.** 2009. Hydrogen production from the monomeric sugars hydrolyzed from hemicellulose by *Enterobacter aerogenes*. Renew Energy **34:**2774–2779. http://dx.doi.org/10.1016/j.renene.2009.04.011.
55. **Ngo TA, Nguyen TH, Bui HTV.** 2012. Thermophilic fermentative hydrogen production from xylose by *Thermotoga neapolitana* DSM 4359. Renew Energy **37:**174–179. http://dx.doi.org/10.1016/j.renene.2011.06.015.
56. **Munro SA, Zinder SH, Walker LP.** 2009. The fermentation stoichiometry of *Thermotoga neapolitana* and influence of temperature, oxygen, and pH on hydrogen production. Biotechnol Prog **25:**1035–1042. http://dx.doi.org/10.1002/btpr.201.